THE JOURNAL OF BIOLOGICAL CHEMISTRY VOL. 291, NO. 36, pp. 18753–18764, September 2, 2016

Gingipains of *Porphyromonas gingivalis* Affect the Stability and Function of Serine Protease Inhibitor of Kazal-type 6 (SPINK6), a Tissue Inhibitor of Human Kallikreins*

Received for publication, March 3, 2016, and in revised form, May 26, 2016 Published, JBC Papers in Press, June 27, 2016, DOI 10.1074/jbc.M116.722942

Karolina Plaza[‡1], Magdalena Kalinska[‡1], Oliwia Bochenska[§], Ulf Meyer-Hoffert[¶], Zhihong Wu[¶], Jan Fischer[¶], Katherine Falkowski[‡], Laura Sasiadek[‡], Ewa Bielecka[‡], Barbara Potempa[‖], Andrzej Kozik[§], Jan Potempa[‡‖2], and Tomasz Kantyka[**]

From the Departments of [‡]Microbiology and [§]Analytical Biochemistry, Faculty of Biochemistry, Biophysics, and Biotechnology, and [**]Malopolska Centre of Biotechnology, Jagiellonian University, 30-387 Krakow, Poland, the [¶]Department of Dermatology, University Clinic Schleswig-Holstein, 24105 Kiel, Germany, and the [‖]Department of Oral Immunology and Infectious Diseases, School of Dentistry, University of Louisville, Louisville, Kentucky 40202

Periodontitis, a chronic inflammation driven by dysbiotic subgingival bacterial flora, is linked on clinical levels to the development of a number of systemic diseases and to the development of oral and gastric tract tumors. A key pathogen, *Porphyromonas gingivalis*, secretes gingipains, cysteine proteases implicated as the main factors in the development of periodontitis. Here we hypothesize that gingipains may be linked to systemic pathologies through the deregulation of kallikrein-like proteinase (KLK) family members. KLKs are implicated in cancer development and are clinically utilized as tumor progression markers. In tissues, KLK activity is strictly controlled by a limited number of tissue-specific inhibitors, including SPINK6, an inhibitor of these proteases in skin and oral epithelium. Here we identify gingipains as the only *P. gingivalis* proteases responsible for SPINK6 degradation. We further show that gingipains, even at low nanomolar concentrations, cleaved SPINK6 in concentration- and time-dependent manner. The proteolysis was accompanied by loss of inhibition against KLK13. We also mapped the cleavage by Arg-specific gingipains to the reactive site loop of the SPINK6 inhibitor. Moreover, we identified a significant fraction of SPINK6-sensitive proteases in healthy saliva and confirmed the ability of gingipains to inactivate SPINK6 under *ex vivo* conditions. Finally, we demonstrate the double-edge action of gingipains, which, in addition, can activate KLKs because of gingipain K-mediated proteolytic processing of the zymogenic proform of KLK13. Altogether, the results indicate the potential of *P. gingivalis* to disrupt the control system of KLKs, providing a possible mechanistic link between periodontal disease and tumor development.

The family of kallikrein proteases (KLKs)[3] contains 15 enzymes that are expressed in many different tissues, suggesting a range of physiological and pathophysiological functions. This diversity of functions is exemplified by the involvement of kallikreins in such processes as normal skin desquamation, psoriatic lesion formation, tooth development, neural plasticity, cancer, and Alzheimer disease (for a review, see Ref. 1). Moreover, kallikreins function in wound healing and proteinase-activated receptor signaling, they process antimicrobial peptides in the epithelial areas, and they affect the stability of some growth factors (2, 3).

KLKs are secreted as inactive proenzymes (pro-KLKs). With the exception of pro-KLK4, all zymogen forms of pro-KLK are then activated in the extracellular milieu by trypsin-like cleavage of the pro-peptide after either an Arg or Lys residue. The activation cleavage is exerted by the kallikrein itself or by still unknown endogenous proteases and constitutes a key mechanism regulating KLK activity in tissues (4).

Kallikrein-specific inhibitors, including some members of the serine protease inhibitor of Kazal-type (SPINK) family, control the activity of KLKs released into tissues (5). To date, at least 10 genes encoding SPINKs were identified in the human genome, and of them, SPINK5, 6, and 9 were reported to control the activity of different KLKs in different tissues. SPINK5 is detected ubiquitously in epithelial tissues and is composed of 15 protease Kazal-type inhibitory domains that inhibit KLK5 and KLK7. It is well known that mutations in the *SPINK5* gene result in elevated activity of epidermal kallikreins and the development of Netherton syndrome, a severe skin disease manifested through abnormal skin desquamation, keratinization, hair follicle defects, and loss of skin barrier function (6). The

* This project was supported by Polish National Centre of Science Research Grants OPUS 2012/05/B/NZ6/00581 (to T. K.), Preludium UMO-2012/07/N/NZ1/00006 (to K. P.), and SYMFONIA UMO-2013/08/W/NZ1/00696 (to J. P.); Polish Ministry of Science and Higher Education Iuventus+ IP2011 022171 (to T. K.) and 2975/7.PR/13/2014/2 (to J. P.); German Research Foundation Grant ME2037/3-3 (to U. M. H.); and Young Scientist Grant for Faculty of Biochemistry, Biophysics, and Biotechnology K/DSC/003271 (to M. K.). The Faculty of Biochemistry, Biophysics, and Biotechnology of the Jagiellonian University in Krakow is a beneficiary of structural funds from the European Union (Grant POIG.02.01.00-12-064/08, "Molecular Biotechnology for Health") and a partner of the Leading National Research Center (KNOW) supported by the Ministry of Science and Higher Education, Poland. The authors declare that they have no conflicts of interest with the contents of this article. The content is solely the responsibility of the authors and does not necessarily represent the official views of the National Institutes of Health.

[1] Both authors contributed equally to this work.

[2] Supported by National Institutes of Health Grants DE 09761 and DE 022597 and European Commission Grant FP7-HEALTH-F3-2012-306029 "TRIGGER"). To whom correspondence should be addressed: Tel.: 48-12-6646343; Fax: 48-12-6646902; E-mail: jan.potempa@uj.edu.pl.

[3] The abbreviations used are: KLK, kallikrein-like proteinase; SPINK, serine protease inhibitor of Kazal-type; ECM, extracellular matrix; AMC, 7-amino-4-methylcoumarin; Tricine, N-[2-hydroxy-1,1-bis(hydroxymethyl)ethyl]glycine.

expression of other SPINK family inhibitors is more tissue-specific. SPINK9 is exclusively found in the palms and soles of the feet (7, 8), and it seems to exclusively inhibit KLK5. In contrast, strongly conserved SPINK6 has a broad spectrum of action that controls kallikrein activity (KLK4, KLK5, KLK12, KLK13, and KLK14) not only in the skin (8, 9) but also in other tissues. This includes the salivary glands, where SPINK6 inhibits KLK5, 6, and 7, and the main salivary kallikrein, KLK13, which comprises 50% of the overall kallikrein activity in the glands (10). Because the reported activity of KLK13 includes degradation of extracellular matrix proteins (11), it is of no surprise that SPINK6 is cross-linked to fibronectin. This increases the local concentration of the inhibitor and protects the extracellular matrix from KLK-mediated damage (12).

An imbalance between SPINK proteins and proteases may cause severe diseases such as pancreatitis, celiac disease, Netherton syndrome, skin barrier defects, and cancer (7, 13–18). Similarly, illegitimate, excessive activation of pro-KLKs by bacterial proteases accompanied by degradation/inactivation of SPINKs may result in damage of an infected connective tissue. This is a likely scenario to occur during progression of periodontitis.

Evidence accumulated to date has strongly implicated the contribution of proteolytic enzymes of subgingival plaque bacteria to the pathogenicity of periodontal disease, the most widespread chronic inflammatory condition in the human host. Importantly, in recent years, periodontal disease has been identified as a significant factor in the development of other systemic diseases, including rheumatoid arthritis, cardiovascular disease, aspiration pneumonia, preterm births, and low birth body weight in infants (19).

The key pathogen implicated in the development of chronic periodontitis is an anaerobic bacterium, *Porphyromonas gingivalis*. *P. gingivalis* secretes three related cysteine proteases, referred to as gingipains, that constitute its main virulence factors. Two gingipains are specific for Arg-Xaa peptide bonds (HRgpA and RgpB), whereas Kgp cleaves after a Lys residue (20). Collectively, gingipains digest a broad spectrum of host proteins to provide the pathogen with nutrients for growth (21). More importantly, gingipains are involved in the disruption of host defense inflammatory reactions and hinder *P. gingivalis* clearance by the immune system (22, 23). This is accomplished by hijacking proinflammatory signaling pathways via cleavage and activation of the proteinase-activated receptor 2 (PAR-2) on human neutrophils (24). Gingipains also affect many host proteolytic systems, affecting the homeostasis of the organism via complex interactions with host proteins, as exemplified by the activation of the kallikrein/kinin pathway and the resultant increase in vascular permeability (25–27). However, activation of tissue prokallikreins, especially locally abundant KLK13, with simultaneous degradation of this protease endogenous inhibitor have not been investigated. This is of significant interest because recent discoveries implicate that infection with oral pathogens may promote tumor progression via facilitation of the epithelial-to-mesenchymal transition and an increase in the malignancy of the tumor (28). Therefore, analysis of the interaction network of pathogen proteases and tumor-related proteinases of the KLK family may provide valuable insights into the mechanistic background of oral infection-cancer correlation.

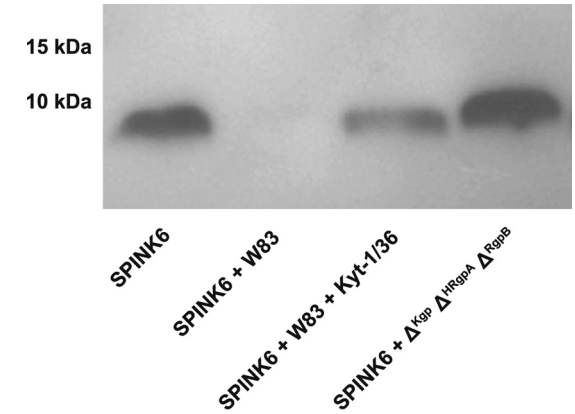

FIGURE 1. **SPINK6 is effectively degraded by *P. gingivalis* bacterial cultures.** SPINK6 (200 ng) was incubated with 10^6 cells of *P. gingivalis* strains for 1 h at 37 °C. The samples were processed for Western blotting using an anti-SPINK6 antibody. Samples of untreated SPINK6, SPINK6 treated with wild-type (W38) bacteria in the presence or absence of inhibitors, and SPINK6 treated with the gingipain triple mutant bacteria (W83$^{\Delta kgp\Delta rgpA\Delta rgpB}$) are shown.

Because SPINK6 is the main inhibitor of salivary kallikreins, especially KLK13, the inactivation of this molecule was our main focus in the context of *P. gingivalis* proteinase-mediated disruption of the KLK-inhibitor balance. Here we present, to our knowledge, the first report of the interplay of the tissue kallikrein system with *P. gingivalis* proteases, further adding to our understanding of the mechanisms of tissue disruption by this widespread oral pathogen.

Results

SPINK6 Is Degraded by P. gingivalis Cultures—P. gingivalis produces many proteolytic enzymes, and, in addition to gingipains, it secretes several other proteases that may interact with SPINK6. Therefore, to investigate the ability of gingipains and other proteases to degrade SPINK6, the inhibitor was preincubated with wild-type *P. gingivalis* W83 in the presence or absence of gingipain-specific inhibitors or with the triple gingipain knockout mutant W83$^{\Delta kgp\Delta rgpA\Delta rgpB}$, completely devoid of gingipain activity (Fig. 1). The wild-type W83 strain completely degraded SPINK6 over the course of the experiment, as indicated by the absence of SPINK6 immunoreactivity on the Western blot of the samples. Preincubation of the W83 strain with Kyt inhibitors that are gingipain-specific, reversible, and do not affect the activity of other proteases, at least at the concentration used (29), protected the majority of SPINK6 from degradation (Fig. 1). Some cleavage of SPINK6 was observed, apparently due to residual activity of the gingipains in the presence of Kyt inhibitors, which were used at low micromolar concentration (5 μM). Exclusive gingipain involvement in degradation was confirmed by the finding that SPINK6 incubation with the triple gingipain mutant W83$^{\Delta kgp\Delta rgpA\Delta rgpB}$ did not affect the stability of the inhibitor. Moreover, when SPINK6 was incubated with another cysteine proteinase of *P. gingivalis*, the streptopain-like TPR, no degradation was observed, even in the presence of a 100 nM concentration of the protease (data not shown). Taken together, these results indicate that wild-type bacteria efficiently

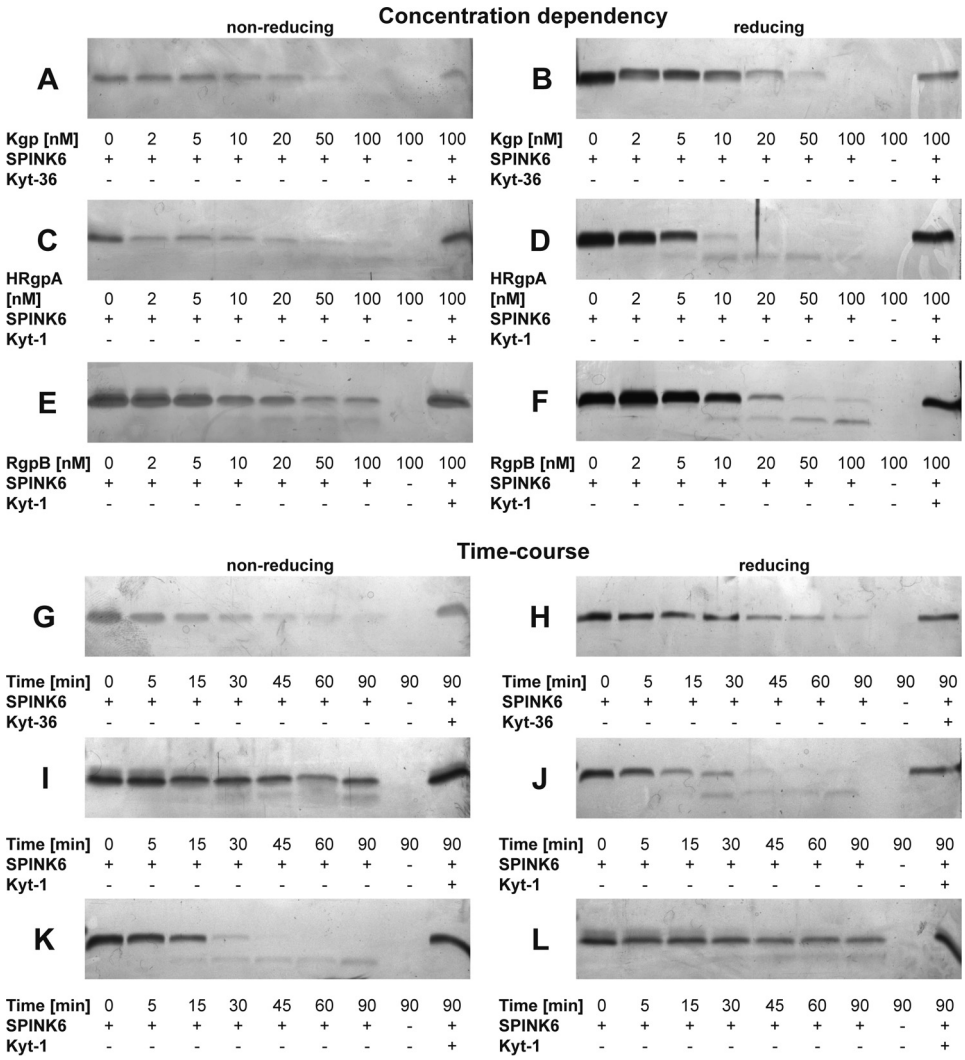

FIGURE 2. **Gingipains degrade SPINK6 in a concentration- and time-dependent manner.** *A–F*, SPINK6 (200 ng) was incubated with the indicated concentration of respective gingipain for 1 h at 37 °C. The reactions were stopped, and the samples were resolved using SDS-PAGE. The gels were silver-stained. All SDS-PAGE separations were performed under reducing and non-reducing conditions. *G–L*, SPINK6 was incubated with 50 nM Kgp, 2 nM RgpB, or 20 nM HRgpA for the indicated times. SDS-PAGE followed by silver staining was used to analyze the degradation.

degrade SPINK6 and that three gingipains (Kgp, RgpB, and HRgpA) are the enzymes responsible for this activity.

Gingipains Degrade SPINK6 in a Time- and Concentration-dependent Manner—P. gingivalis gingipains degraded SPINK6 in a concentration-dependent (Fig. 2, *A–F*) and time-dependent (Fig. 2, *G–L*) dependent manner. The Lys-specific gingipain Kgp (20 nM) degraded SPINK6 nearly completely, as visualized by silver-staining SDS-PAGE gels. By contrast, SPINK6 appeared intact on non-reducing gels following incubation with Arg-specific gingipains, even at relatively high enzyme concentrations (10 nM RgpB and 50 nM HRgpA). However, SDS-PAGE under reducing conditions revealed the accumulation of the lower molecular weight proteolysis product during incubation with 2 nM RgpB and 10 nM HRgpA.

Similarly, the time course analysis showed progressive degradation by Kgp (50 nM) with no significant differences between reducing and non-reducing conditions. After 45 min, only traces of the native inhibitor could be detected by SDS-PAGE. Incubation with the Arg-specific gingipains led to the accumulation of the nicked inhibitor, represented by two polypeptide chains resolved only by reducing SDS-PAGE. For both RgpB (2 nM) and HRgpA (20 nM), a 30-min incubation was long enough for almost complete cleavage of the inhibitor. Cumulatively, these results are congruent with the gingipain specificities and the SPINK6 structure, which contains six Lys residues scattered throughout the polypeptide chain and only a single Arg residue at the P1 position in the reactive site loop of the inhibitor stabilized by three disulfide bridges.

Gingipain-treated SPINK6 Is Inactive as a KLK13 Inhibitor— The reactive site loop of SPINK6 is stabilized by three disulfide bridges that hold in close proximity the P1 Arg and P1′ Glu residues. Because Kazal inhibitors nicked at the P1-P1′ bond may retain inhibitory activity (30), we tested the ability of gingipain-treated SPINK6 to inhibit KLK13 (Fig. 3). The results indicated that the apparently stable, Rgps-nicked SPINK6 displayed no inhibitory activity when incubated in a 2:1 molar ratio with KLK13, in contrast to the intact inhibitor, which diminished KLK13 activity by ~90%.

Limited Proteolysis of SPINK6 by Gingipains—To further characterize SPINK6 interactions with gingipains, the cleavage

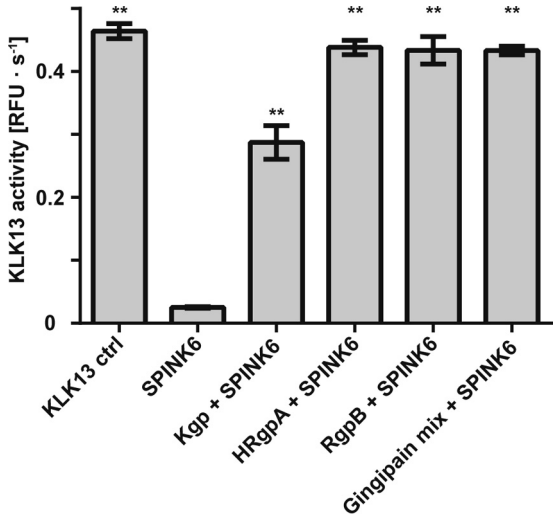

FIGURE 3. **Gingipain degradation leads to loss of the inhibitory properties of SPINK6.** SPINK6 was incubated for 1 h at 37 °C with each of the indicated gingipains (20 nM) or with a mixture of all three gingipains (4 nM each). The reactions were stopped by addition of 5 μM Kyt-1 and/or Kyt-36, and KLK13 was added to the samples. KLK13 activity was measured using the fluorogenic substrate Boc-VPR-AMC. Results were normalized to the uninhibited KLK13 as 100% and compared with SPINK6 incubated alone. Statistical significance: **, $p < 0.05$. *RFU*, relative fluorescence unit.

sites within the inhibitor were identified. As suggested by SDS-PAGE analysis, reverse-phase HPLC chromatography of Kgp-treated SPINK6 (Fig. 4*A*) confirmed the complete fragmentation of the inhibitor. Six discrete fragments of the SPINK6 polypeptide chain generated by Kgp were identified, resulting from the four Lys-Xaa peptide bond cleavages as identified by MS/MS analysis (Fig. 4*G*). As expected, none of the degradation products showed any inhibitory activity toward the KLK13 protease (Fig. 4*D*).

The pattern of degradation products for the Arg-specific HRgpA and RgpB differed significantly from that of Kgp. Five main peaks were identified (Fig. 4, *B* and *C*), and none of them contained the unmodified inhibitor. All of the products were consistent with a single cleavage after Arg^{42}. Importantly, the SPINK6 structure is stabilized by three disulfide bridges that keep the polypeptide fragments together after cleavage with gingipains. However, 2 mM L-cysteine required for gingipains activity reduced the disulfide bridges in the SPINK6 molecule already destabilized by a proteolytic cleavage. In the case of multiple cleavages of the inhibitor polypeptide chain by Kgp, there were no intact bridges left to keep the fragments together. Conversely, a single cleavage at Arg^{42} by Rgps generated predominantly the double-chain, full-length molecule, as demonstrated by the +18-Da mass shift compared with the native unmodified inhibitor. However, in an unstable two-chain structure of SPINK6, disulfide bridges holding the molecule together must be partially reduced, yielding N- ($SPINK6_{1-42}$) and C-terminal ($SPINK6_{43-80}$) fragments. It can be speculated that the rearrangement of the disulfide bridges in these fragments during sample preparation for HPLC analysis led to two different molecular conformations of identical mass (MS/MS data) but differed in the retention times on HPLC (Fig. 4, *H* and *I*). Nonetheless, the fragmentation of the inhibitor chain seems to be required, as the intact inhibitor was unaffected by 2 mM L-cysteine used in the assay and eluted as a single peak, retaining the full inhibitory activity.

To test for residual activity among the cleavage products, the inhibitory potential of all of the Kgp-, RgpB-, and HRgpA-derived products was evaluated (Fig. 4, *D–F*). Peak areas were used to calculate the amount of peptide in each peak. Reactions were carried out under more rigorous conditions than previous assays, using a 10:1 molar ratio of the given inhibitor fragment to KLK13 (compared with the 2:1 molar ratio in the experiments above). The N-terminal $SPINK6_{1-42}$ and the C-terminal $SPINK6_{43-80}$ fragments were completely inactive as inhibitors, whereas the full-length, +18-Da, single hydrolysis-modified peptide displayed 50% inhibitory activity of the control SPINK6 when incubated with KLK13 under the same reaction conditions. This result indicates that this product is a relatively weak KLK13 inhibitor, as a 10-fold molar excess did not fully inhibit the target enzyme compared with native SPINK6, which inhibited 90% of the protease activity at a 2:1 molar ratio in the experiments above.

SPINK6 Acts as a Potentially Important Inhibitor in Human Saliva—Human saliva displays a significant, trypsin-like proteolytic activity. As SPINK6 remains cross-linked to the ECM and provides localized inhibitory protection, the fraction of saliva activity susceptible to the SPINK6 control was estimated. Hence, a saliva mixture from five healthy individuals was titrated with recombinant SPINK6 using the Boc-Val-Pro-Arg-AMC fluorogenic substrate. Saliva (5 μl) was diluted to a final volume of 200 μl (40-fold dilution), and proteolytic activity was measured in the presence of 0–100 nM SPINK6 (Fig. 5*B*). In addition, the susceptibility of the saliva of each individual was tested separately (Fig. 5*A*). The 50 nM SPINK6 was able to inhibit ~60% of trypsin-like activity in each of the individual saliva samples. Moreover, the Arg-specific proteinase activity in the saliva mixture decreased in a SPINK6 concentration-dependent manner until 75% reduction. Nonetheless, ~25% of the trypsin-like activity in the tested sample remained unaffected by SPINK6. The overall SPINK6-sensitive activity was determined as ~1 μM in the undiluted saliva by SPINK6 active site titration (data not shown). This result indicates that inactivation of SPINK6 could render a major fraction of protease activity uncontrolled, with the potential to disrupt signaling pathways and damage tissues.

Kgp Activates pro-KLK13—The majority of the kallikrein family proteases contain an Arg or Lys residue at the profragment cleavage site (31) and, therefore, may be susceptible to activation by gingipains. Because KLK13 contains a Lys residue at the activation site, the ability of Kgp, a Lys-specific gingipain, to generate the mature form of the protease was tested (Fig. 6). Increasing concentrations of Kgp were incubated with pro-KLK13, and KLK13 activity was measured using the Boc-Val-Pro-Arg-AMC substrate (Fig. 6*A*), which is not hydrolyzed by Kgp. To ensure that no HRgpA/RgpB contamination affected the results, the assay was performed in the presence of the Rgps inhibitor Kyt-1. As shown in Fig. 7*A*, Kgp activated proKLK13 in a concentration-dependent manner, with a maximal effect at 5 nM Kgp. Further increases in Kgp concentration (50 and 100 nM) resulted in a gradual loss of activity that could be the result of degradation of the mature KLK13 by high concentrations of

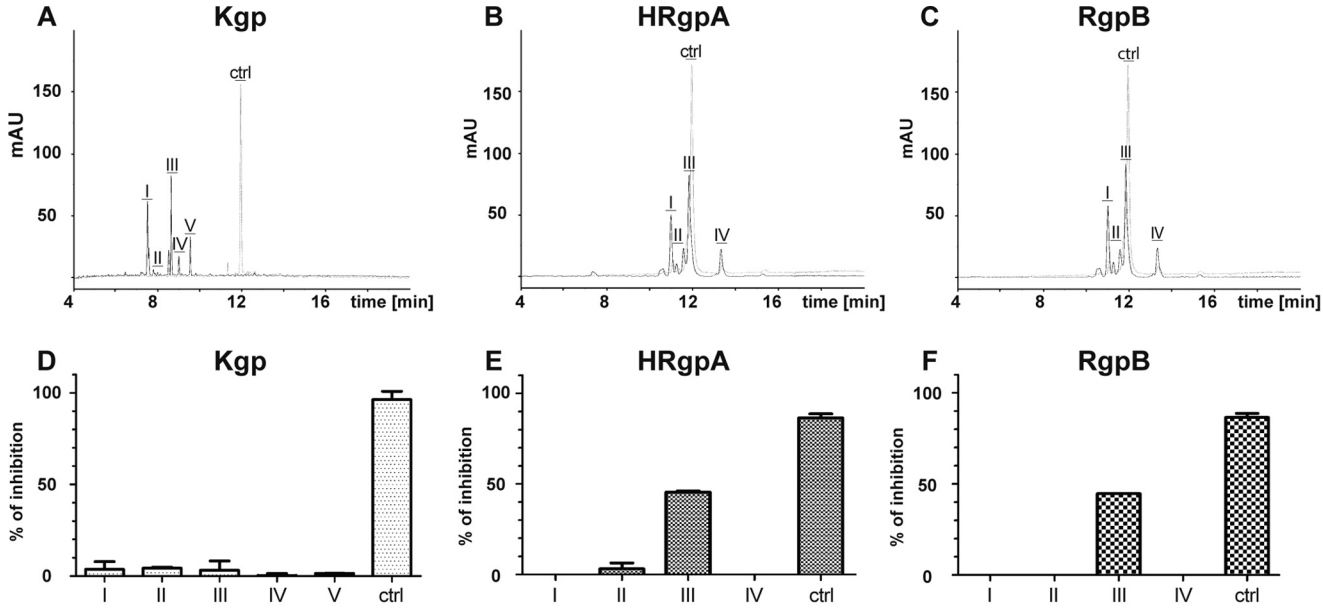

G Kgp

Frac.	Retention time [min]	Average mass [Da]	Assigned sequence
I	7.51	1629.7	TYGNKCAFCKAIVKS
I	7.57	2313.1	$_{(K37)}$VYCTRESNTHCGSDGQTYGN**K**$_{58}$
II	8.01	878.6	$_{(K71)}$ISLKHPGK79
III	8.54	568.2	$_{(K58)}$CAFC**K**$_{63}$
III	8.70	1967.9	YVEFHHHHHHDDDD**K**$_{23}$
IV	9.00	1510.7	n.d.
V	9.60	1948.9	TRESNTHCGSDGQTYGN**K**$_{58}$

H HRgpA

Frac.	Retention time [min]	Average mass [Da]	Assigned sequence
I	10.99	4081.6	YVEFHHHHHHDDDDKQGGQVD CGEFQDPKVYCT**R**$_{42}$
II	11.25	4081.6	YVEFHHHHHHDDDDKQGGQVD CGEFQDPKVYCT**R**$_{42}$
II	11.58	3947.0	$_{(R42)}$ESNTHCGSDGQTYGNKCAFC KAIVKSGGKISLKHPGKC
III	11.84	8029.4	YVEFHHHHHHDDDDKQGGQVD CGEFQDPKVYCT**R**$_{42}$ESNTHC GSDGQTYGNKCAFCKAIVKSGG KISLKHPGKC **+ H_2O**
IV	13.33	3947.0	$_{(R42)}$ESNTHCGSDGQTYGNKCAFC KAIVKSGGKISLKHPGKC

I RgpB

Frac.	Retention time [min]	Average mass [Da]	Assigned sequence
I	11.01	4081.6	YVEFHHHHHHDDDDKQGGQVD CGEFQDPKVYCT**R**$_{42}$
II	11.26	4081.6	YVEFHHHHHHDDDDKQGGQVD CGEFQDPKVYCT**R**$_{42}$
II	11.58	3947.0	$_{(R42)}$ESNTHCGSDGQTYGNKCAFC KAIVKSGGKISLKHPGKC
III	11.85	8029.4	YVEFHHHHHHDDDDKQGGQVD CGEFQDPKVYCT**R**$_{42}$ESNTHC GSDGQTYGNKCAFCKAIVKSGG KISLKHPGKC **+ H_2O**
IV	13.33	3947.0	$_{(R42)}$ESNTHCGSDGQTYGNKCAFC KAIVKSGGKISLKHPGKC

FIGURE 4. **Gingipains target the reactive site loop of SPINK6.** SPINK6 (10 μg) was incubated with 100 nM Kgp, RgpB, or HRgpA for 1 h at 37 °C. The reactions were stopped by acidification with TFA (0.1% final concentration), and the samples were resolved by HPLC (*A–C*). Eluted peaks were pooled, tested for their inhibitory activity against KLK13 (*D–F*), and analyzed by MS (*G–I*). *Ctrl*, control. *AU*, absorbance units; *Frac.*, fraction.

gingipains. Nonetheless, the activity was fairly stable, leaving ~80% of maximal KLK13 activity even at 100 nM Kgp. Similarly, the active site labeling by FP-biotin indicated the proper binding of the biotinylated inhibitor, as presented in Fig. 6*B*. Increasing concentrations of Kgp resulted in the appearance of the band, corresponding to the active KLK13. Already at 0.1 nM Kgp concentration, binding of the FP-biotin was visible, and with further increases up to 30 nM Kgp, the band was saturated. Finally, the activation of KLK13 by Kgp was confirmed by the removal of the N-terminal His tag attached to the KLK13 profragment (Fig. 6*C*). Similarly, the Western blotting analysis using anti-His tag antibody revealed a decrease in the signal with increasing Kgp concentration, resulting in near-complete disappearance of the respective band at 50 nM Kgp concentration. This indicates that increasing concentrations of Kgp indeed facilitate the removal of the N-terminal profragment in the nanomolar range of concentrations and, coupled with the activity and FP-biotin labeling results, confirm the ability of Kgp to activate KLK13 and to release a functional protease. This indicates that low nanomolar levels of Kgp activate proKLK13, disrupting the protease-inhibitor balance already affected by SPINK6 proteolytic inactivation by gingipains.

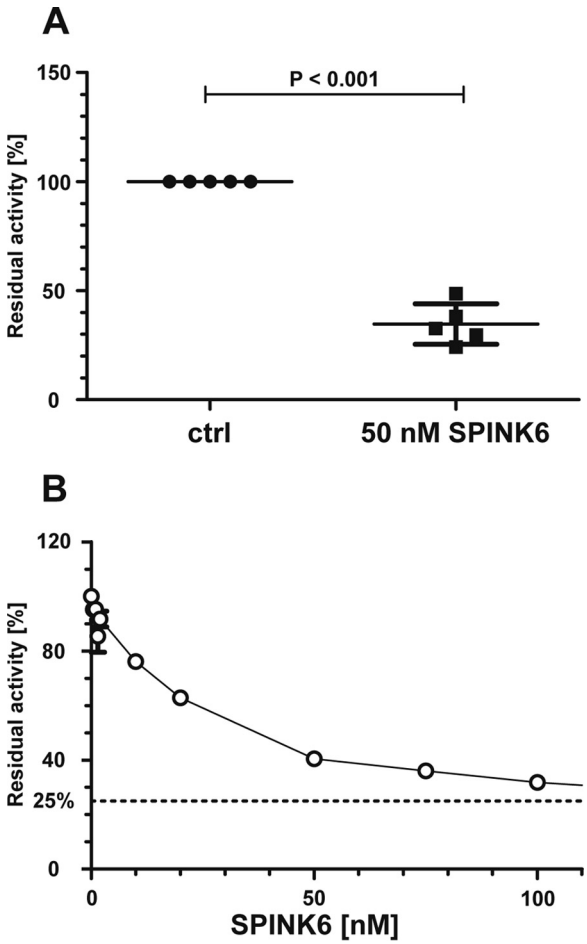

FIGURE 5. **The majority of trypsin-like proteinase activity in healthy saliva is sensitive to SPINK6 inhibition.** *A*, saliva of each healthy individual (5 μl, $n = 5$) was diluted 40× in reaction buffer, and 50 nM SPINK6 was added to each sample. Activity was measured using the fluorescent trypsin substrate Boc-Val-Pro-Arg-AMC. The results were normalized, and activity in the SPINK6-untreated sample was set as the 100% control (*ctrl*) for each individual. Significantly different means were identified using Mann-Whitney test. *B*, the saliva mixture from healthy individuals (5 μl) was diluted 40× in reaction buffer and incubated with increasing concentrations of recombinant SPINK6. Residual trypsin-like protease activity was measured using the Boc-Val-Pro-Arg-AMC substrate and was plotted as percent of control sample activity (no inhibitor added). Data are presented as mean ± S.D.

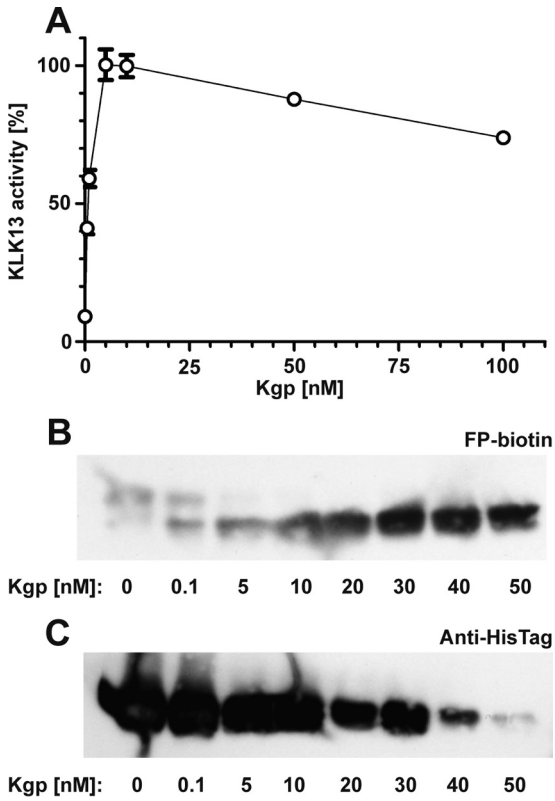

FIGURE 6. **Lys-specific gingipain K activates pro-KLK13.** Pro-KLK13 was incubated with the indicated concentrations of Kgp in the presence of the Arg-specific gingipain inhibitor Kyt-1 for 1 h at 37 °C. *A*, after incubation, samples were diluted into Boc-Val-Pro-Arg-AMC solution, and the rate of substrate hydrolysis was measured. Results were plotted as percent of maximal KLK13 activity *versus* Kgp concentration. *B*, Western blotting analysis of pro-KLK13 incubated with increasing concentrations of Kgp, followed by active site labeling by FP-biotin, results in appearance of a band corresponding to active KLK13. *C*, Western blotting analysis with anti-His tag antibodies shows the removal of the N-terminal His tag upon incubation with Kgp in a dose-dependent manner.

Gingipains Degrade SPINK6 in the Presence of Saliva—Finally, the *in vivo* environment contains not only saliva but numerous other proteins, possibly acting as competing substrates for gingipains. Therefore, the degradation of SPINK6 was analyzed in the presence of 25% saliva (a mixture from five healthy volunteers). SPINK6 (10 μg) was incubated for 1 h with 50 nM gingipains in the presence of the 25% saliva mixture diluted in reaction buffer. Samples were analyzed by Western blotting with anti-His tag antibodies. Additionally, the residual inhibitory activity of the degradation mixture was verified using the KLK13 inhibition assay (Fig. 7*A*). Western blotting results (Fig. 7*B*) confirmed the superior activity of the Arg-specific HRgpA and RgpB, which were able to completely degrade 10 μg of SPINK6 in the presence of 25% saliva. Similarly, the presence of HRgpA or RgpB blocked inhibition by SPINK6 because >60% of KLK13 activity in saliva was restored. Kgp again was proven to be the least effective, with residual levels of SPINK6 detected by Western blotting and only 15% of KLK13 activity restored. These data indicate that Arg-specific gingipains may specifically target SPINK6 in the complex protein mixture, whereas Kgp degradation could be regarded as a rather nonspecific attack on the exposed Lys residues, limited by the presence of other saliva-derived proteins.

Discussion

Our results indeed confirm the ability of *P. gingivalis* to affect the kallikrein-inhibitor balance, adding to the well known pathological interactions of this bacterium with the protease control system of the host. Biochemical and mutant strain analyses using healthy saliva mixtures *in vitro* showed that gingipains were the sole proteases responsible for this activity. Gingipain concentrations in the nanomolar range were effective, and a combination of gingipains was found to be most efficient. Moreover, the Lys-specific Kgp not only degraded the inhibitor but was also capable of activating the proform of KLK13, as opposed to Arg-specific HRgpA and RgpB.

This important observation indicates that gingipains indeed possess the potential to activate the main kallikrein proteinase, KLK13, present in human saliva (32). Additionally, our results confirm the ability of gingipains (both Lys- and Arg-specific) to activate other members of KLK family of proteases, an obser-

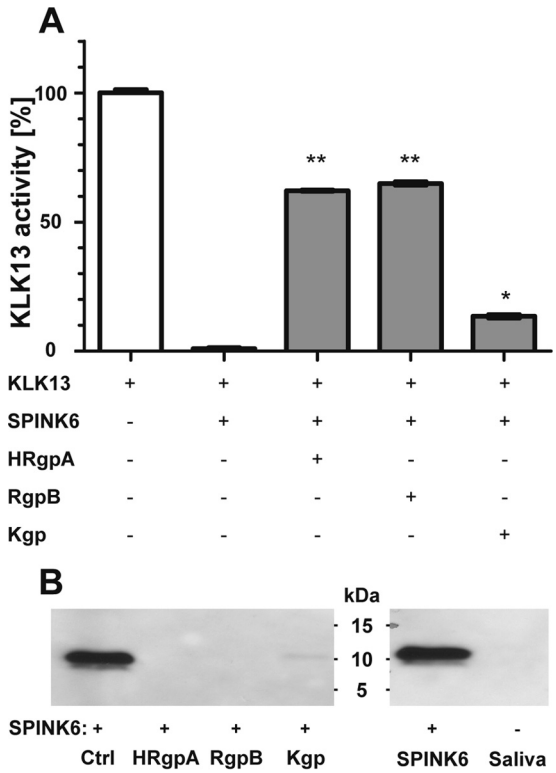

FIGURE 7. **Gingipains affect SPINK6 integrity and function in the presence of saliva.** SPINK6 (10 μg) was incubated with a 25% saliva mixture from five healthy donors in the presence of the indicated gingipain (50 nM). After 1 h, the reaction was stopped by addition of gingipain-specific inhibitors and analyzed. *A*, the ability of the reaction products to inhibit KLK13 was evaluated in 25% saliva in the presence of gingipain inhibitors. A 2-fold molar excess of the SPINK6 reaction products was added to KLK13 solution, and activity was measured using fluorescent monitoring of the Boc-VPR-AMC substrate. *B*, Western blotting analysis with anti-His tag antibodies shows that HRgpA and RgpB fully degraded SPINK6. Kgp was less active, leaving a small fraction of the inhibitor intact. *Ctrl*, control. Statistical significance: *, $p < 0.01$; **, $p < 0.05$.

vation pursued in our future work.[4] Moreover, the complex protein mixture present in saliva did not block the inactivation of SPINK6 by Arg-specific gingipains, indicating a targeted activity of these pathogen-derived proteinases.

Additionally, our results indicate a substantial level of salivary trypsin-like activity, of which 75% is susceptible to SPINK6-mediated inhibition. This allows the estimation of the total KLK activity in saliva approximating 1 μM, an amount left uncontrolled after the SPINK6 inactivation. Taken together, these data indicate that the kallikrein-inhibitor balance is one of the targets of *P. gingivalis* proteases in producing inflammation.

Gingipains are well established virulence factors of *P. gingivalis* and are often described as an archetype of protease involvement in bacterial virulence. These aggressive enzymes, with strict P1 specificity toward Arg (HRgpA and RgpB) or Lys (Kgp) residues, target a number of essential components of human immunity, coagulation cascade, and regulatory pathways (33). Their impact on host protease-inhibitor systems has been reported previously, as gingipains inactivate the α_1-protease inhibitor (34), secretory leukocyte peptidase inhibitor (35), and, as reported previously by our group, elafin (36). The common feature of the aforementioned inhibitors is that all three, working in concert, control the proteolytic activity released from neutrophils and, thus, prevent damage of connective tissue during inflammation. This report provides evidence that gingipains can efficiently degrade SPINK6, a Kazal-type inhibitor of the tissue kallikrein family of proteinases. To our knowledge, this is the first example of the gingipain-mediated disruption of a system that controls the activity of these tissue-specific enzymes.

All three gingipains are capable of inactivation of SPINK6. As the sequence of SPINK6 (Fig. 8) contains six Lys residues, it is not surprising that Lys-specific gingipain K was able to fragment the protein into small peptides unable to inhibit the target enzyme. More importantly, however, cleavage by Arg-specific HRgpA and RgpB also led to the loss of inhibitor activity. SPINK6 contains only a single Arg residue, located in the P1 position of the reactive site loop. Moreover, the disulfide bridges in the polypeptide stabilize the inhibitor against dissociating into separate fragments (Fig. 8). Several reports indicate that these inhibitors can maintain their function after cleavage of the P1-P1′ peptide bond, possibly with lowered efficiency (37). Indeed, as mass spectrometry analysis confirmed that the main product of HRgpA or RgpB degradation of SPINK6 was the nicked inhibitor with the reactive site loop held together by disulfide bridges, and this polypeptide retained partial inhibitory activity. Two other peptides were identified, fragments $SPINK6_{1-42}$ and $SPINK6_{43-80}$, both with the oxidized disulfide bridges, and were inactive as proteinase inhibitors. Each fragment eluted from an HPLC column with two distinct retention times and with the oxidized ("bound") disulfide bridge state. Therefore, as the MS/MS sequence analysis confirmed the identity of these peptides, we hypothesize that the distinct elution times for each of the peptide fragments correspond to the different disulfide bridge configurations within the given fragment.

As cysteine proteinases, gingipains are dependent on reducing agents in the reaction buffer, and, thus, it is possible that reorganization of the disulfide bridges is the result of the initial reduction of the protein. Nevertheless, our data confirm full activity of SPINK6 under optimized experimental conditions with buffer containing 2 mM L-cysteine (data not shown). Moreover, all control samples in the experiments were incubated in reaction buffer and, as confirmed by HPLC and MS, maintained full activity with no changes in the structure or disulfide bridges. Therefore, we conclude that reorganization of the disulfide bridge pattern is most likely a result of internal instability in the cleaved inhibitor. This model is in agreement with the standard mechanism of inhibition where a target protease forms a pocket tightly binding the inhibitor and preventing its free dissociation, hence stabilizing the cleaved form in the binding cleft. By contrast, hydrolysis by gingipain R may allow release of the internal tension of the molecule by disulfide bridge reorganization. As mentioned above, this hypothesis is supported by the detected state of disulfide bridges in the isolated peptides that, despite 2 mM L-cysteine in the reaction buffer, were all oxidized.

[4] K. Plaza, M. Kalinska, O. Bochenska, U. Meyer-Hoffert, Z. Wu, J. Fischer, K. Falkowski, L. Sasiadek, E. Bielecka, B. Potempa, A, Kozik, J. Potempa, and T. Kantyka, unpublished results.

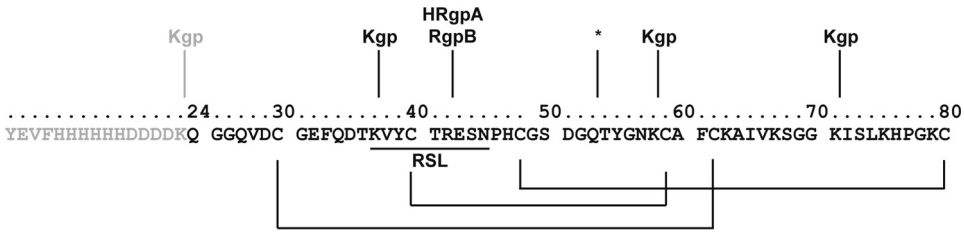

FIGURE 8. **SPINK6 is cleaved by gingipains.** Kgp cleavage was detected at four positions: on the C-terminal side of $Lys^{(24-1)}$, Lys^{37}, Lys^{58}, and Lys^{71} (numbering of the full-length SPINK6 according to the Uniprot database). The hydrolysis after $Lys^{(24-1)}$ is located at the enterokinase cleavage site in the N-terminal extension of the protein (*gray*). All other Kgp recognition sites are within the sequence of the native SPINK6 protein. HRgpA and RgpB hydrolyze the single peptide bond on the C-terminal side of Arg^{42}. An additional unassigned hydrolysis site at Gln^{53} is marked (*asterisk*) and may be an artifact of the MS analysis. The disulfide bond scaffold binds N-terminal and C-terminal regions of the molecule, hence dissociation of the $SPINK6_{1-42}$ and $SPINK6_{43-72}$ requires reorganization of the disulfide bridges.

The inactivation of SPINK6, a potent, tightly binding inhibitor of kallikrein family proteinases (10), is an important observation. SPINK6 is present in epithelial tissues, including skin and gingiva, in two forms: fully soluble and transglutaminated by its N-terminal glutamine to extracellular matrix proteins, like fibronectin (data not shown and Ref. 12). This diversification of the inhibitor forms provides protection for the extracellular matrix, locally increasing the inhibitory capacity because of covalent linkage of the active inhibitor to the ECM proteins. As suggested for other tightly binding tissue inhibitors of proteases (*e.g.* elafin (38)), the protective system is constituted by the initial response molecule, a tightly binding, locally produced inhibitor, which later transfers the protease molecule onto the final, serum-derived, irreversible inhibitor (either serpin or α_2-macroglobulin). Hence, the tightly binding inhibitor provides the necessary quick response and protects essential components of the tissue. The fact that gingipains not only inactivate SPINK6, as presented here, but are also capable of direct degradation of ECM proteins (39) likens them to an enzymatic arsenal that is capable of both inactivation of host protease inhibitors and degradation of the ECM matrix itself.

Tissue kallikreins are a family of 15 extracellular serine proteases with trypsin- and chymotrypsin-like specificity. Their functions are not well defined, but recent studies indicate that kallikreins 5, 7, and 14 regulate epithelial desquamation (40); KLK3, 7, and 13 may activate plasminogen; and KLK2, KLK3, KLK6, KLK7, and KLK14 may degrade ECM proteins (as reviewed in Refs. 41 and 42). Moreover, KLK5 and KLK7 are enzymes that process both precursor and mature forms of antimicrobial cathelicidine hCAP18 in the skin (3), and KLK5 and KLK14 regulate inflammation through activation of proteinase-activated receptors (43). Furthermore, our results implicate KLK13, one of the main salivary kallikreins, as an important enzyme in the regulation of epithelial wound healing, most likely via processing of the growth factor precursors.[4] Additionally, kallikreins have been implicated in numerous reports as important factors and biomarkers in the development and progression of tumors (as reviewed in Ref. 44).

Interestingly, the development of periodontitis and bacterial infections of the oral cavity have been linked to an increased risk of oral cancer (45, 46). More recent reports further strengthen the correlation between *P. gingivalis* infection and oral and stomach cancer development *in vitro* and *in vivo* (28, 47). This effect is usually attributed to the direct effect of bacterial toxins and virulence factors promoting the development of chronic inflammation. Our results propose a novel explanation of the periodontitis-cancer correlation. The inactivation of a kallikrein-specific inhibitor may be beneficial for bacteria, as it affects inflammation, tissue reconstruction, and antimicrobial-peptide processing; however, the long-term increase in kallikrein activity could eventually lead to the development of oral cancer via activation of growth factors, facilitation of chronic inflammation, and promotion of metastasis by ECM matrix remodeling.

Our report provides evidence for the involvement of *P. gingivalis* gingipains in destabilization of the regulation of KLK activity through inactivation of SPINK6, the epithelium-specific inhibitor of kallikreins. This result not only adds to the known tendency of *P. gingivalis* to disrupt the proteolytic balance in infected tissues but also provides a possible mechanistic link between the development of periodontitis and oral cancer progression. As the role of the salivary kallikreins in the development of oral cancer is not known, the reported data provide a basis for further investigation of *P. gingivalis* infection and kallikreins in carcinogenesis and tumor metastasis in the oral cavity.

Experimental Procedures

The *Pichia pastoris* expression system was obtained from Invitrogen. Gingipains and proKLK13 were purified as described previously (48, 49). As HRgpA and Kgp were purified from whole culture medium, cross-contamination was possible. Therefore, the Arg gingipain-specific (Kyt-1) and Lys gingipain-specific (Kyt-36) (29) small molecule, tightly binding inhibitors were used in all gingipain experiments to ensure inhibition of undesired cross-reactivity in the samples. All reagents were obtained from Sigma-Aldrich (Taufkirchen, Germany) unless otherwise indicated.

Expression and Purification of Recombinant SPINK6—A DNA sequence encoding SPINK6 (GenBank accession no. GQ504704.1) was amplified from keratinocyte cDNAs in three consecutive PCR reactions that introduced an EcoRI cleavage site and histidine tag- and enterokinase cleavage site-coding sequence at the 5′ end and a NotI recognition site at the 3′ end. The final amplicon was ligated into the pPIC9 vector following the α-factor secretion sequence and used to transform *Escherichia coli* strain Dh5α. Positive clones were sequenced to verify the sequence, and the plasmid was linearized with SalI (Thermo Scientific) and electrotransformed into *P. pastoris* strain GS115 to obtain the Mut^+ phenotype. Following addition of 1 M sor-

bitol, cells were plated on MD plates (1.34% yeast nitrogen base, 0.00004% biotin, and 2% glucose) and grown for 48 h at 30 °C. The Mut^+ phenotype was verified by the ability to grow in the presence of methanol. Positive recombinants were chosen for expression cultures. BMGY medium (1% yeast extract, 2% peptone, 1.34% yeast nitrogen base, 1% ammonium sulfate, 0.0004% biotin, 100 nM potassium phosphate buffer (pH 6.0), and 1% glycerol) was inoculated with a single colony and incubated at 30 °C for ~16 h with shaking (250 rpm), and, after reaching $A_{600} = 4.0$, the cells were harvested by centrifugation (5 min, 3000 RCF) and resuspended in BMMY medium (1% yeast extract, 2% peptone, 1.34% yeast nitrogen base, 1% ammonium sulfate, 0.0004% biotin, 100 nM potassium phosphate buffer (pH 6.0), and 0.5% methanol) at $A_{600} = 1.0$ to induce expression. Cultures were incubated for 72 h at 30 °C with shaking at 250 rpm for protein production. Every 24 h, aliquots of 100% methanol were added to maintain 0.5% final concentration. Cells were then harvested by centrifugation (15 min, 3000 RCF), and the supernatant was collected, filtered, and mixed with 50 mM sodium phosphate buffer (pH 7.5), 2.5 M NaCl, and 25 mM imidazole at a ratio of 4:1 (supernatant:buffer, v:v). Finally, equilibrated nickel-Sepharose resin (GE Healthcare) was added and incubated with the supernatant for 16 h at 4 °C with gentle agitation. Histidine-tagged protein was eluted with increasing concentrations of imidazole. The fraction of interest was then acidified by adding TFA to a final concentration of 0.1%. The sample was loaded onto an equilibrated, semi-preparative HPLC column (Jupiter C18, 5 μm, 10/100 mm, Phenomenex). Protein was eluted using a 25–35% gradient of phase B (0.08% TFA, 80% acetonitrile) in 17 column volumes using an ÄktaMicro chromatography unit (GE Healthcare). Fractions containing the inhibitor were collected and dried using a CentriVap concentrator (Labconco) to remove the solvent.

Degradation of SPINK6 by Bacterial Cultures—*P. gingivalis* wild-type W83 and $W83^{\Delta kgp\Delta rgpA\Delta rgpB}$ strains were cultured overnight in Schaedler medium supplemented with hemin (1 mg/ml), vitamin K (0.5 mg/ml), and cysteine (0.05 mg/ml) under anaerobic conditions (90% N_2, 5% CO_2, 5% H_2) at 37 °C. Overnight cultures were diluted into fresh medium to $A_{600} = 0.1$ and cultured as above until reaching $A_{600} = 1.0$. Subsequently, 200 ng of SPINK6 was added to 1×10^6 bacteria in culture medium and incubated under anaerobic conditions for 1 h at 37 °C. The reaction was terminated by addition of SDS-PAGE sample buffer containing DTT and boiling for 5 min. The products of the reaction were separated by SDS-PAGE, and proteins were electrotransferred onto a PVDF membrane (Immobilon-P, Millipore). The membrane was blocked with 3% skim milk in TTBS buffer (50 mM Tris-HCl (pH 7.5), 500 mM NaCl, and 0.05% Tween 20) for 1 h at 37 °C. The blocked membrane was incubated overnight at 4 °C with primary antibody (1:1000, goat anti-human SPINK6, purified as described before (8)) and then washed four times with TTBS and incubated with a secondary antibody (HRP-conjugated anti-goat IgG (1:30,000, catalog no. A8919, Sigma) for 1 h at room temperature. Pierce ECL (Thermo Fisher Scientific) was used as the chemiluminescence substrate, and images were developed using Medical X-Ray-Film Blue (Agfa).

Analysis of SPINK6 Degradation—Before each experiment, gingipains (HRgpA, RgpB, and Kgp) were activated for 15 min at 37 °C in TNCT buffer (0.2 M Tris-HCl, 0.15 M NaCl, 5 mM $CaCl_2$, and 0.05% Tween 20 (pH 7.5)) supplemented with 10 mM L-cysteine. For analysis of concentration dependence, SPINK6 (200 ng) was incubated with 0, 2, 5, 10, 20, 50, or 100 nM of each gingipain for 1 h at 37 °C in TNCT buffer containing 2 mM L-cysteine. The reaction was terminated by addition of Kyt-1 or Kyt-36 (PeptaNova GmbH, Sandhausen, Germany), which specifically inhibit R- or K-type gingipains, respectively (5 μM final concentration). Samples were separated by SDS-PAGE and silver-stained. Based on the results obtained, concentrations of gingipains were chosen to perform the time course analysis of SPINK6 degradation. For the degradation time course, SPINK6 (200 ng) was incubated with activated Kgp (50 nM), RgpB (2 nM), or HRgpA (20 nM) for 0, 5, 15, 30, 45, 60, or 90 min at 37 °C in TNCT buffer supplemented with 2 mM L-cysteine. After the indicated time intervals, the reaction was stopped by addition of Kyt-1 or Kyt-36 to samples with R- or K-type gingipains, respectively. Samples were resolved using SDS-PAGE, and protein bands were visualized by silver staining.

SDS-PAGE—Samples for separation by SDS-PAGE were prepared under reducing and non-reducing conditions. In both cases, sample buffer (4% SDS, 60% glycerol, 0.3 M Tris (pH 8.0), and 0.01% bromphenol blue) was added to reaction mixtures at a 1:3 volume ratio. For reducing conditions, sample buffer was supplemented with 100 mM DTT, and samples were boiled for 5 min at 100 °C. Electrophoresis was run in a Schagger/von Jagow Tricine system with a two-layer separating gel: 16% (T:C 8.7:1) and 10% (T:C 16.5:1). Protein size was estimated using the PageRuler Plus prestained protein ladder (Fermentas) after silver staining.

Inhibition Assays—SPINK6 (40 nM) was incubated with each gingipain (20 nM) or with an equimolar mixture of three gingipains, each at 4 nM final concentration for 1 h at 37 °C in a total volume of 50 μl of TNCT containing 2 nM L-cysteine. The reactions were terminated by the addition of 5 μl of Kyt-1 or Kyt-36 to samples with R or K gingipains, respectively, or both into samples of SPINK6 incubated with the mixture of gingipains and the KLK13 control (4.5 μM final concentration of each Kyt). After incubation for 15 min at 37 °C, 45 μl of KLK13 in TNET buffer (100 mM Tris, 150 mM NaCl, 5 mM EDTA, and 0.05% Tween 20 (pH 7.5)) was added, and samples were incubated for another 15 min at 37 °C. The final concentration of enzymes, inhibitors, and substrate (in 100 μl of reaction mixture) was 20 nM SPINK6, 10 nM gingipains (or 2 nM each gingipain in a mixture), 20 nM KLK13, and 2.4 μM Kyt inhibitor. Finally, 100 μl of a fluorogenic substrate, N-t-Boc-Val-Pro-Arg-AMC (40 μM, Sigma) in TNET buffer was added, and hydrolysis of the substrate was recorded for 60 min as the increase of fluorescence intensity (an excitation wavelength of 355 nm and an emission wavelength of 460 nm) using a microplate fluorescence reader (SpectraMax Gemini EM, Molecular Devices). Of note, the kinetic parameters of substrate hydrolysis by KLK13 were determined previously: $K_m = 10.5 \times 10^{-5} \pm 1.7 \times 10^{-5}$ M and $k_{cat}/K_m = 4.66 \times 10^3\ s^{-1}\cdot M^{-1}$.

HPLC Separation and Analysis of Degradation Products—SPINK6 (10 μg) was incubated with 100 nM Kgp, RgpB, or HRgpA in TNCT buffer containing 2 mM L-cysteine for 1 h at

37 °C. The reaction was stopped by acidification of the samples with TFA (0.1% final concentration (v/v)). Samples (100 μl) were loaded onto a column equilibrated with 0.1% TFA (AERIS C18 peptide, 3.6 μm, 4.6/150 mm, Phenomenex). Elution was performed using a 10–80% gradient of phase B (0.08% TFA, 80% acetonitrile) in 19 column volumes. Collected fractions were dried using a CentriVap concentrator (Labconco). Each fraction was resuspended in TNET buffer to a final concentration of 1 μM based on the peak integration data. The sample (20 nM final concentration) was then mixed with KLK13 (2 nM final concentration) and incubated in TNET buffer for 15 min at 37 °C (100-μl total volume). Subsequently, 40 μM substrate was added (100 μl), and fluorescence intensity was measured as described above. The final mixture contained 10 nM SPINK6 or its degradation products, 1 nM KLK13 (10:1 molar ratio), and 20 μM substrate in a final volume of 200 μl.

MS Analysis of the Degradation Products—Peptide fractions were dried by evaporation, redissolved in 30% methanol supplemented with 0.1% (v/v) formic acid, and analyzed using an HTC Ultra ETD II mass spectrometer (Bruker) equipped with an electrospray ionization source and an ion trap analyzer. The samples were directly injected using a syringe pump (KD Scientific) at a flow rate of 180 μl/h and analyzed in positive ion mode with a capillary voltage of 3.5 kV, a nebulizer pressure of 10 psi, a drying gas flow of 5 liters/min, and an ion source temperature of 300 °C. Spectra were acquired in MS and MS/MS modes in the range of 100–3000 m/z with three different fragmentation types: collision-induced dissociation, collision-induced dissociation/electron transfer dissociation, or electron transfer dissociation/proton transfer reaction. MS data were processed manually using the DataAnalysis™ 4.0 and Biotools™ 3.2 software.

Activation of pro-KLK13 with Kgp—Kgp was activated in TNCT buffer supplemented with 10 mM L-cysteine for 15 min at 37 °C. A sample of 200 nM pro-KLK13 (expressed in *P. pastoris*) was incubated with 0, 0.5, 1, 5, 10, 50, or 100 nM Kgp in TNCT containing 2 mM L-cysteine and 5 μM Kyt-1 for 1 h at 37 °C. The reactions were terminated by addition of Kyt-36 (5 μM) to inhibit Kgp. After 15-min incubation, 40 μM N-t-Boc-Val-Pro-Arg-AMC substrate was added, and fluorescence intensity was recorded as described above. The final mixture contained 100 nM pro-KLK13/KLK13, 1 nM Kgp, 1 μM Kyt-1, 1 μM Kyt-36, and 20 μM substrate in TNET buffer (200-μl total volume). Simultaneously, to verify the formation of the functional active site of KLK13 and to monitor removal of the N-terminal His tag, a separate reaction was performed. Pro-KLK13 (2 μg, 3.5 μM) was incubated with 0, 0.1, 5, 10, 20, 40, or 50 nM of activated Kgp in TNCT buffer containing 2 mM L-cysteine for 1 h at 37 °C. The reactions were terminated as described above. These samples were divided, and the first set of samples (0.5 μg of proKLK13) was incubated with 1 μM FP-biotin (Santa Cruz Biotechnology Inc.) for 30 min at 37 °C. The second set containing 1 μg of proKLK13 was used for an anti-His tag Western blot. Both sets of samples were separated by SDS-PAGE and electrotransferred onto a PVDF membrane (Immobilon-P, Millipore). Nonspecific binding sites were blocked with 5% BSA in TTBS. The FP-biotin-labeled samples were incubated with HRP-conjugated streptavidin (Sigma-Aldrich) diluted 1:25,000 in TTBS. Similarly, the second set of samples was developed using a monoclonal, HRP-conjugated anti-His tag antibody (catalog no. A7058, Sigma-Aldrich) diluted 1:20,000 in TTBS. After incubation, the antibodies were washed, and bands were visualized as described above.

Titration of Trypsin-like Activity in the Saliva—Saliva collected from five healthy individuals was pooled. The mixture was centrifuged for 30 min at 12,000 × *g*, and 5 μl of supernatant was diluted 10-fold in 45 μl of TNET buffer on a microtiter plate. To wells containing diluted saliva, 50 μl of solution containing 0, 2, 8, 20, 40, 80, 200, or 400 nM SPINK6 was added. After a 15-min preincubation, 100 μl of 40 μM N-t-Boc-Val-Pro-Arg-AMC substrate was added, and residual trypsin-like activity was measured. In addition, separate saliva samples from healthy donors were incubated with 50 nM SPINK6 and analyzed, as above, to provide information about individual variations in SPINK6-sensitive protease content.

Degradation of SPINK6 in the Presence of Saliva—Saliva was clarified by centrifugation as described above and diluted 2-fold with sterile PBS. Gingipains were preactivated in TNCT buffer supplemented with 10 mM reduced L-cysteine (Sigma-Aldrich) for 15 min at 37 °C. To eliminate potential cross-contamination of Rgp with Kgp and vice versa, Kyt inhibitors (2 μM final concentration) were added to eliminate any contaminating activity: Kyt-1 to the Kgp sample and Kyt-36 to the HRgpA and RgpB samples. SPINK6 (10 μg) was incubated with each gingipain (50 nM final concentration) in the presence of 25% saliva (a mixture of five healthy donor samples) for 1 h in 37 °C in TNCT buffer containing 2 mM cysteine. The reaction was stopped by adding Kyt-1 or Kyt-36 (2 μM final concentration) into samples with HRgpA/RgpB or Kgp, respectively, and incubating at 37 °C for 5 min. The integrity of SPINK6 was determined by both Western blotting analysis and by its ability to inhibit the enzymatic activity of KLK13. Samples separated by SDS-PAGE were transferred onto PVDF (Bio-Rad). Nonspecific binding sites were blocked with 5% skim milk in TTBS, followed by incubation with a monoclonal HRP-conjugated anti-His tag antibody (catalog no. A7058, Sigma-Aldrich) diluted 1:20,000 in TTBS. Alternatively, a 2-fold molar excess of the reaction products (as estimated by the original SPINK6 amount in the sample) was added to a 10 nM KLK13 solution in 0.1 M Tris-HCl (pH 7.5) supplemented with 2 μM Kyt-1 and Kyt-36. Kallikrein activity was measured by monitoring the fluorescence intensity as described above.

Author Contributions—K. P. and M. K. performed the majority of the experimental work. K. P. performed the inhibition and degradation experiments, and M. K. was responsible for human saliva preparation and analysis. K. P. and M. K. participated in the preparation of the manuscript. O. B. and A. K. performed the mass spectrometry experiments and data analysis. U. M. H., Z. W., and J. F. were responsible for isolation of the SPINK6 gene and establishment of the expression system of the inhibitor. K. F., L. S., and E. B. performed expression and purification of recombinant (pro)KLK13. B. P. was responsible for purification of the bacterial gingipains. J. P. and T. K. were equally responsible for the experimental design, data analysis, work coordination, and preparation of the manuscript.

References

1. Kalinska, M., Meyer-Hoffert, U., Kantyka, T., and Potempa, J. (2016) Kallikreins: the melting pot of activity and function. *Biochimie* **122,** 270–282

2. Gao, L., Chao, L., and Chao, J. (2010) A novel signaling pathway of tissue kallikrein in promoting keratinocyte migration: activation of proteinase-activated receptor 1 and epidermal growth factor receptor. *Exp. Cell Res.* **316,** 376–389
3. Yamasaki, K., Schauber, J., Coda, A., Lin, H., Dorschner, R. A., Schechter, N. M., Bonnart, C., Descargues, P., Hovnanian, A., and Gallo, R. L. (2006) Kallikrein-mediated proteolysis regulates the antimicrobial effects of cathelicidins in skin. *FASEB J.* **20,** 2068–2080
4. Yousef, G. M., and Diamandis, E. P. (2002) Expanded human tissue kallikrein family: a novel panel of cancer biomarkers. *Tumour Biol.* **23,** 185–192
5. Mägert, H. J., Ständker, L., Kreutzmann, P., Zucht, H. D., Reinecke, M., Sommerhoff, C. P., Fritz, H., and Forssmann, W. G. (1999) LEKTI, a novel 15-domain type of human serine proteinase inhibitor. *J. Biol. Chem.* **274,** 21499–21502
6. Walley, A. J., Chavanas, S., Moffatt, M. F., Esnouf, R. M., Ubhi, B., Lawrence, R., Wong, K., Abecasis, G. R., Jones, E. Y., Harper, J. I., Hovnanian, A., and Cookson, W. O. (2001) Gene polymorphism in Netherton and common atopic disease. *Nat. Genet.* **29,** 175–178
7. Brattsand, M., Stefansson, K., Hubiche, T., Nilsson, S. K., and Egelrud, T. (2009) SPINK9: a selective, skin-specific Kazal-type serine protease inhibitor. *J. Invest. Dermatol.* **129,** 1656–1665
8. Meyer-Hoffert, U., Wu, Z., Kantyka, T., Fischer, J., Latendorf, T., Hansmann, B., Bartels, J., He, Y., Gläser, R., and Schröder, J. M. (2010) Isolation of SPINK6 in human skin: selective inhibitor of kallikrein-related peptidases. *J. Biol. Chem.* **285,** 32174–32181
9. Fischer, J., Wu, Z., Kantyka, T., Sperrhacke, M., Dimitrieva, O., Koblyakova, Y., Ahrens, K., Graumann, N., Baurecht, H., Reiss, K., Schröder, J. M., Proksch, E., and Meyer-Hoffert, U. (2014) Characterization of Spink6 in mouse skin: the conserved inhibitor of kallikrein-related peptidases is reduced by barrier injury. *J. Invest. Dermatol.* **134,** 1305–1312
10. Kantyka, T., Fischer, J., Wu, Z., Declercq, W., Reiss, K., Schröder, J. M., and Meyer-Hoffert, U. (2011) Inhibition of kallikrein-related peptidases by the serine protease inhibitor of Kazal-type 6. *Peptides* **32,** 1187–1192
11. Kapadia, C., Ghosh, M. C., Grass, L., and Diamandis, E. P. (2004) Human kallikrein 13 involvement in extracellular matrix degradation. *Biochem. Biophys. Res. Commun.* **323,** 1084–1090
12. Fischer, J., Koblyakova, Y., Latendorf, T., Wu, Z., and Meyer-Hoffert, U. (2013) Cross-linking of SPINK6 by transglutaminases protects from epidermal proteases. *J. Invest. Dermatol.* **133,** 1170–1177
13. Witt, H., Luck, W., Hennies, H. C., Classen, M., Kage, A., Lass, U., Landt, O., and Becker, M. (2000) Mutations in the gene encoding the serine protease inhibitor, Kazal type 1 are associated with chronic pancreatitis. *Nat. Genet.* **25,** 213–216
14. Gasiorowska, A., Talar-Wojnarowska, R., Czupryniak, L., Smolarz, B., Romanowicz-Makowska, H., Kulig, A., and Malecka-Panas, E. (2011) The prevalence of cationic trypsinogen (PRSS1) and serine protease inhibitor, Kazal type 1 (SPINK1) gene mutations in Polish patients with alcoholic and idiopathic chronic pancreatitis. *Dig. Dis. Sci.* **56,** 894–901
15. Hoefnagel, J. J., Dijkman, R., Basso, K., Jansen, P. M., Hallermann, C., Willemze, R., Tensen, C. P., and Vermeer, M. H. (2005) Distinct types of primary cutaneous large B-cell lymphoma identified by gene expression profiling. *Blood* **105,** 3671–3678
16. Stenman, U. H. (2011) Role of the tumor-associated trypsin inhibitor SPINK1 in cancer development. *Asian J. Androl.* **13,** 628–629
17. Tüysüz, B., Ojalvo, D., Mat, C., Zambruno, G., Covaciu, C., Castiglia, D., and D'Alessio, M. (2010) A new SPINK5 donor splice site mutation in siblings with Netherton syndrome. *Acta Dermato-Venereologica* **90,** 95–96
18. Rockett, J. C., Patrizio, P., Schmid, J. E., Hecht, N. B., and Dix, D. J. (2004) Gene expression patterns associated with infertility in humans and rodent models. *Mutat. Res.* **549,** 225–240
19. Olsen, I., and Potempa, J. (2014) Strategies for the inhibition of gingipains for the potential treatment of periodontitis and associated systemic diseases. *J. Oral Microbiol.* **6,** 24800
20. Imamura, T. (2003) The role of gingipains in the pathogenesis of periodontal disease. *J. Periodontol.* **74,** 111–118
21. Potempa, J., Sroka, A., Imamura, T., and Travis, J. (2003) Gingipains, the major cysteine proteinases and virulence factors of *Porphyromonas gingivalis*: structure, function and assembly of multidomain protein complexes. *Curr. Protein Pept. Sci.* **4,** 397–407
22. Uehara, A., Naito, M., Imamura, T., Potempa, J., Travis, J., Nakayama, K., and Takada, H. (2008) Dual regulation of interleukin-8 production in human oral epithelial cells upon stimulation with gingipains from *Porphyromonas gingivalis*. *J. Med. Microbiol.* **57,** 500–507
23. Guo, Y., Nguyen, K. A., and Potempa, J. (2010) Dichotomy of gingipains action as virulence factors: from cleaving substrates with the precision of a surgeon's knife to a meat chopper-like brutal degradation of proteins. *Periodontology 2000* **54,** 15–44
24. Ford, P. J., Gamonal, J., and Seymour, G. J. (2010) Immunological differences and similarities between chronic periodontitis and aggressive periodontitis. *Periodontology 2000* **53,** 111–123
25. Imamura, T., Potempa, J., Pike, R. N., Moore, J. N., Barton, M. H., and Travis, J. (1995) Effect of free and vesicle-bound cysteine proteinases of *Porphyromonas gingivalis* on plasma clot formation: implications for bleeding tendency at periodontitis sites. *Infect. Immun.* **63,** 4877–4882
26. Imamura, T., Potempa, J., Pike, R. N., and Travis, J. (1995) Dependence of vascular permeability enhancement on cysteine proteinases in vesicles of *Porphyromonas gingivalis*. *Infect. Immun.* **63,** 1999–2003
27. Imamura, T., Pike, R. N., Potempa, J., and Travis, J. (1994) Pathogenesis of periodontitis: a major arginine-specific cysteine proteinase from *Porphyromonas gingivalis* induces vascular permeability enhancement through activation of the kallikrein/kinin pathway. *J. Clin. Invest.* **94,** 361–367
28. Ha, N. H., Woo, B. H., Kim da, J., Ha, E. S., Choi, J. I., Kim, S. J., Park, B. S., Lee, J. H., and Park, H. R. (2015) Prolonged and repetitive exposure to *Porphyromonas gingivalis* increases aggressiveness of oral cancer cells by promoting acquisition of cancer stem cell properties. *Tumour Biol.* **36,** 9947–9960
29. Kadowaki, T., Baba, A., Abe, N., Takii, R., Hashimoto, M., Tsukuba, T., Okazaki, S., Suda, Y., Asao, T., and Yamamoto, K. (2004) Suppression of pathogenicity of *Porphyromonas gingivalis* by newly developed gingipain inhibitors. *Mol. Pharmacol.* **66,** 1599–1606
30. Rawlings, N. D., Tolle, D. P., and Barrett, A. J. (2004) Evolutionary families of peptidase inhibitors. *Biochem. J.* **378,** 705–716
31. Yoon, H., Laxmikanthan, G., Lee, J., Blaber, S. I., Rodriguez, A., Kogot, J. M., Scarisbrick, I. A., and Blaber, M. (2007) Activation profiles and regulatory cascades of the human kallikrein-related peptidases. *J. Biol. Chem.* **282,** 31852–31864
32. Shaw, J. L., and Diamandis, E. P. (2007) Distribution of 15 human kallikreins in tissues and biological fluids. *Clin. Chem.* **53,** 1423–1432
33. Imamura, T., Travis, J., and Potempa, J. (2003) The biphasic virulence activities of gingipains: activation and inactivation of host proteins. *Curr. Protein Pept. Sci.* **4,** 443–450
34. Meyer, J., Guessous, F., Huynh, C., Godeau, G., Hornebeck, W., Giroud, J. P., and Roch-Arveiller, M. (1997) Active and α-1 proteinase inhibitor complexed leukocyte elastase levels in crevicular fluid from patients with periodontal diseases. *J. Periodontol.* **68,** 256–261
35. Into, T., Inomata, M., Kanno, Y., Matsuyama, T., Machigashira, M., Izumi, Y., Imamura, T., Nakashima, M., Noguchi, T., and Matsushita, K. (2006) Arginine-specific gingipains from *Porphyromonas gingivalis* deprive protective functions of secretory leucocyte protease inhibitor in periodontal tissue. *Clin. Exp. Immunol.* **145,** 545–554
36. Kantyka, T., Latendorf, T., Wiedow, O., Bartels, J., Gläser, R., Dubin, G., Schröder, J. M., Potempa, J., and Meyer-Hoffert, U. (2009) Elafin is specifically inactivated by RgpB from *Porphyromonas gingivalis* by distinct proteolytic cleavage. *Biol. Chem.* **390,** 1313–1320
37. Laskowski, M., and Qasim, M. A. (2000) What can the structures of enzyme-inhibitor complexes tell us about the structures of enzyme substrate complexes? *Biochim. Biophys. Acta* **1477,** 324–337
38. Guyot, N., Zani, M. L., Maurel, M. C., Dallet-Choisy, S., and Moreau, T. (2005) Elafin and its precursor trappin-2 still inhibit neutrophil serine proteinases when they are covalently bound to extracellular matrix proteins by tissue transglutaminase. *Biochemistry* **44,** 15610–15618
39. Potempa, J., Banbula, A., and Travis, J. (2000) Role of bacterial proteinases in matrix destruction and modulation of host responses. *Periodontology 2000* **24,** 153–192

40. Simon, M., Jonca, N., Guerrin, M., Haftek, M., Bernard, D., Caubet, C., Egelrud, T., Schmidt, R., and Serre, G. (2001) Refined characterization of corneodesmosin proteolysis during terminal differentiation of human epidermis and its relationship to desquamation. *J. Biol. Chem.* **276,** 20292–20299
41. Lundwall, A., and Brattsand, M. (2008) Kallikrein-related peptidases. *Cell. Mol. Life Sci.* **65,** 2019–2038
42. Kontos, C. K., and Scorilas, A. (2012) Kallikrein-related peptidases (KLKs): a gene family of novel cancer biomarkers. *Clin. Chem. Lab. Med.* **50,** 1877–1891
43. Stefansson, K., Brattsand, M., Roosterman, D., Kempkes, C., Bocheva, G., Steinhoff, M., and Egelrud, T. (2008) Activation of proteinase-activated receptor-2 by human kallikrein-related peptidases. *J. Invest. Dermatol.* **128,** 18–25
44. Borgoño, C. A., and Diamandis, E. P. (2004) The emerging roles of human tissue kallikreins in cancer. *Nat. Rev. Cancer* **4,** 876–890
45. Tezal, M., Grossi, S. G., and Genco, R. J. (2005) Is periodontitis associated with oral neoplasms? *J. Periodontol.* **76,** 406–410
46. Tezal, M., Sullivan, M. A., Hyland, A., Marshall, J. R., Stoler, D., Reid, M. E., Loree, T. R., Rigual, N. R., Merzianu, M., Hauck, L., Lillis, C., Wactawski-Wende, J., and Scannapieco, F. A. (2009) Chronic periodontitis and the incidence of head and neck squamous cell carcinoma. *Cancer Epidemiol. Biomark. Prev.* **18,** 2406–2412
47. Gao, S., Li, S., Ma, Z., Liang, S., Shan, T., Zhang, M., Zhu, X., Zhang, P., Liu, G., Zhou, F., Yuan, X., Jia, R., Potempa, J., Scott, D. A., Lamont, R. J., Wang, H., and Feng, X. (2016) Presence of *Porphyromonas gingivalis* in esophagus and its association with the clinicopathological characteristics and survival in patients with esophageal cancer. *Infect. Agents Cancer* **11,** 3
48. Potempa, J., and Nguyen, K. A. (2007) Purification and characterization of gingipains. *Curr. Protoc. Protein Sci.* **Chapter 21,** Unit 21 20
49. Kapadia, C., Chang, A., Sotiropoulou, G., Yousef, G. M., Grass, L., Soosaipillai, A., Xing, X., Howarth, D. H., and Diamandis, E. P. (2003) Human kallikrein 13: production and purification of recombinant protein and monoclonal and polyclonal antibodies, and development of a sensitive and specific immunofluorometric assay. *Clin. Chem.* **49,** 77–86